FINITE ELEMENT DELAMINATION STUDY OF A NOTCHED COMPOSITE PLATE UNDER FLEXURAL LOADS

A. André[1,2], S. Nilsson[1] and L.E. Asp[1,3]
[1]Swerea Sicomp AB, SE-431 22 Mölndal, Sweden, alann.andre@swerea.se
[2]Div. of Structural Engineering, Chalmers University of Technology, SE-41296 Göteborg, Sweden
[3]Div. of Polymer Engineering, Luleå University of Technology, SE-97187 Luleå, Sweden

ABSTRACT

The delamination process in notched composite plates under flexural loading has been investigated using finite element analysis. Cohesive elements implemented in the commercial finite element package ABAQUS have been used in the region around the drilled-hole, and positioned between layers where delamination was observed during experiments presented in an accompanying paper. The delamination initiation and subsequent propagation was studied between the layers at the tension side separately and simultaneously. For all FE models, the load displacement curve was in good agreement with the one from experiments. However, the amount of damage reported from the fractography study was more extensive than that predicted by the models. Finally, it was shown that the models with only one cohesive layer show significantly different results to that of the model with four cohesive layers in terms of size of the degradation area.

Keywords: Damage tolerance, interlaminar, cohesive element

INTRODUCTION

The use of composite materials for structural parts in the aeronautic industry has increased tremendously during the last decade. Composite materials are brittle materials sensitive to stress concentration from notches or damage. In particular, composites are sensitive to out-of-plane loads causing delaminations [1]. During the design process of a fibre composite structural part, its damage tolerance behaviour must be considered for mainly three reasons: to assure the integrity of the part and the safety of the aircraft, to anticipate failure and to avoid unnecessary replacement of a part which can still fulfil its structural function. Therefore, studies have focused on the understanding and prediction of the mechanisms of damage initiation and propagation in notched composite [1], and on implementing reliable tools in commercial finite element codes to model these composite structures [2-3].

The objective of this study is to determine the delamination initiation and propagation in notched composite laminates under flexural loading. The commercial finite element package ABAQUS [4] is used to carry out the investigation. The study focuses on the efficient use of commercial cohesive element to model ply delamination in notched composite laminates. This study will address delamination as the only damage

mechanism. The results from the finite element analysis are compared to experimental results of four-point bending tests performed in [5] for validation.

INTERLAMINAR DAMAGE MODEL WITH COHESIVE ELEMENTS

Cohesive elements implemented in ABAQUS [4] are a powerful tool to model delamination onset and growth in composite materials. The theoretical background is well described in [4] and [2]. The use of cohesive elements together with a bilinear traction separation law (TSL, Figure 1) is outlined below.

The debonding or delamination processes of composite material occur in two main steps: damage initiation and damage propagation.

The cohesive laws for mode I and II capture the linear elastic and softening behaviour before fracture, and can be obtained by performing Double Cantilever Beam tests and End Notched Flexural beam tests.

Cohesive elements can be defined by a linear elastic response, a strength criteria and a damage evolution law based on energies. The damage initiates when a quadratic stress criterion is fulfilled ($\delta = \Delta^0$), see equation (1). The strength of the composite in the normal and shear directions are used as input data,

$$\left(\frac{\sigma_{33}}{\hat{\sigma}_{33}}\right)^2 + \left(\frac{\tau_{13}}{\hat{\tau}_{13}}\right)^2 + \left(\frac{\tau_{23}}{\hat{\tau}_{23}}\right)^2 = 1 \tag{1}$$

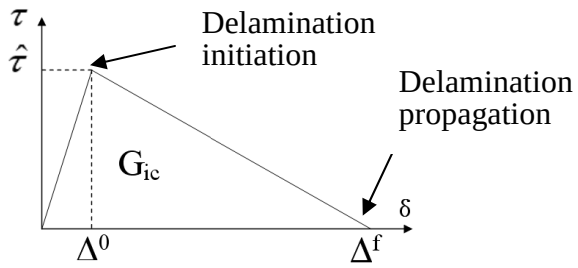

Figure 1. Bilinear traction separation law.

The damage evolution is governed by a damage parameter which describes the rate of stiffness softening after damage initiation ($\delta = \Delta^0$). The damage propagation ($\delta = \Delta^f$) is studied in terms of energy release rate and fracture toughness. To accurately predict delamination growth for mode I, mode II loading condition [2], the Benzeggagh-Kenane criteria are used [3], as expressed in equation (2).

$$G_{Ic} + \left(G_{IIc} - G_{Ic}\right)\left(\frac{\beta}{1+2\beta^2-2\beta}\right)^{\eta} = G_{mc} \text{ , with } \beta = \frac{\Delta_{shear}}{\Delta_{peel} + \Delta_{shear}} \tag{2}$$

where G_{Ic} and G_{IIc} are the fracture toughness in mode I and II respectively. The exponent η is chosen to 1.45. β is the parameter determining the mixed mode ratio based on the current values of the peel and shear opening in the TSL for mode I and II respectively.

SPECIMENS GEOMETRY AND MATERIALS

Specimens geometry

The geometry of the drilled composite plates is shown in Figure 2. The thickness of the plate is 4.16 mm. The laminate is quasi-isotropic with the lay-up $[(0/90/+45/-45)_4]_{S32}$. The ply thickness is 0.13 mm. The test specification and the manufacturing of specimens were performed by Saab Aerostructures.

Experiments have been carried out on similar specimens with a support span of 390 mm instead of 410 mm [5]. However, one specimen had a support span of 410 mm and the loading was stopped before total failure to carry out a fractographic analysis. Therefore, to allow analysis of the interrupted test, a support span of 410 mm was modelled.

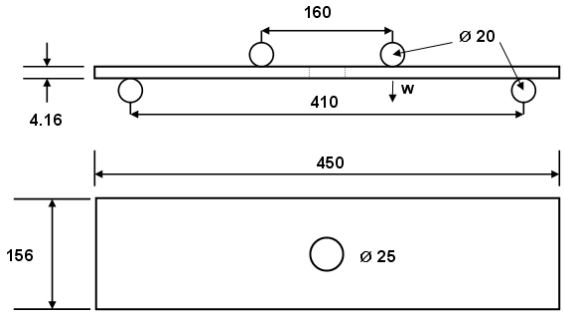

Figure 2. Geometry of the notched composite plate (mm)

Materials

The material used was Hexcel HTA/6376C carbon fibre epoxy unidirectional prepreg. The mechanical properties of the ply are reported in Table 1. The values in Table 1 and 2 are approximate.

Table 1. HTA/6376C - Mechanical properties

Composites: Engineering constants ([GPa] (except Poisson's ratios))									
	E_{11}	E_{22}	E_{33}	G_{12}	G_{13}	G_{23}	υ_{12}	υ_{13}	υ_{23}
HTA/6376C	140	10	10	5.0	5.0	3.0	0.30	0.30	0.50

The material parameters for the cohesive layer are reported in Table 2. The stiffness of the elastic part of the traction separation laws is calculated using the stiffness of the composite and the thickness of the cohesive layer [4].

Table 2. Cohesive layer properties

Interface: Cohesive properties			
$\hat{\sigma}$ **(MPa)**	$\hat{\tau}$ **(MPa)**	G_{Ic} **(J/m^2)**	G_{IIc} **(J/m^2)**
20	30	300	700

FINITE ELEMENT MODEL

Element type, mesh, boundary condition and applied load

The model was divided into a maximum of 12 different parts: two roller supports, a composite laminate part with a cut in the vicinity of the hole, 5 composite laminate parts in the vicinity of the hole and the cohesive layers were inserted between the layers where delaminations were observed [5].

The elements used in the FE-models are reported in Table 3:

Table 3. Elements type and number

	Cohesive layer	**Composite laminate around the hole**	**Composite laminate**	**Support**
Element type	Cohesive COH3D8	Continuum shell SC8R	Continuum shell SC8R	Linear brick C3D8R
Number	3276	3276	7352	1392

The mesh and the assembly of the different parts considered in the model are shown in Figure 3 below. All parts were joined by surface to surface tie constraints.

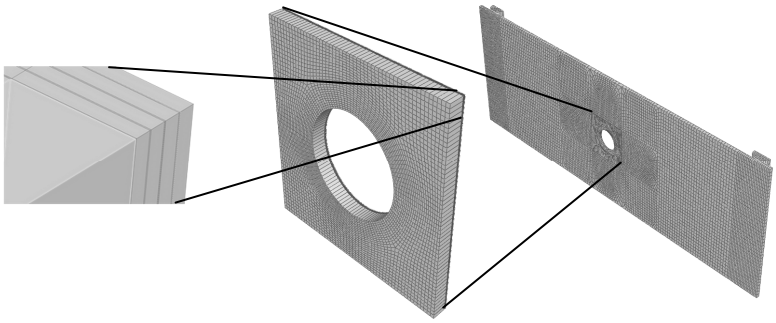

Figure 3. Mesh of the whole model

To reduce the computing time, symmetry is often used to model a half or a quarter of composite laminates loaded in bending. The quasi-isotropic lay-up considered in this study does not offer this possibility because of the unsymmetrical ± 45° layers.

The loading was applied through a controlled displacement of 80 mm. All nodal displacements on the bottom surface of the roller support were restrained.

Assumption and particular settings

The roller supports used on the 4-point bending experiments are often neglected in FE models and replaced by boundary conditions restricting nodal displacement along the contact line. Due to large displacements during the experiments (deflection over 80 mm) and large sliding of the specimen on the roller supports this assumption is invalid as it does not capture the correct reaction forces. Consequently, the roller support has to be modelled explicitly. This introduces a cost demanding contact

interaction in the FE-model. Since the objective is to determine the delamination onset and growth, the contacts were defined with a coarse mesh to decrease the computing time. In ABAQUS, the interaction “composite laminate – steel support” was defined using a finite sliding formulation together with a node to surface discretization method. Non linear effects due to large deformations were taken into account in the FE-model.

Damage models where material softening occurs are often generating convergence difficulties in ABAQUS standard. Therefore, it is useful to include artificial damping in the model in order to overcome these problems. In all models, a damping value of 3.10^{-4} was used. By comparison of the viscous damping energy with the total strain energy, it was verified that the artificial damping does not yields inaccurate solutions.

Method

Four models employing one cohesive layer were analysed. In these models, the cohesive layer was positioned at the first interface on the tension side in the first model, at the second interface in the second model, and so on.

In a fifth model cohesive layers were placed at the first four interfaces on the tension side, see Figure 4.

Model 1, with cohesive elements at the first interface, i.e. between the 0° and 90° layers on the tension loaded side, has been run with 3 different element sizes for the cohesive elements: 0.5 mm, 0.25 mm and 0.125 mm.

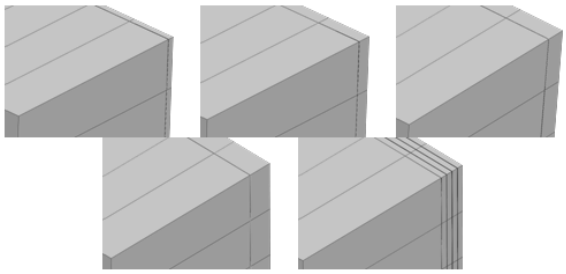

Figure 4. The five models with cohesive elements positioned at different composite layer interfaces on the tension side

RESULTS

Structural response

The experimental result for the 410 mm load span specimen reported in [5] is presented in Figure 5-a.

The computed load displacement curves for all five models are plotted in Figure 5-b. The deflection *w* was recorded at a node at the compression side under the loading line (see Figure 2) and the load was recorded at the support. Due to the large deformation, the x-component of the load increases significantly under loading.

It can be seen that there is no difference between the 5 models in terms of load-deflection behaviour of the specimen in bending. The maximum load obtained from FE models is 3.8 kN (at w = 80 mm), which is in good agreement with the experimental result of 3.9 kN at the same deflection.

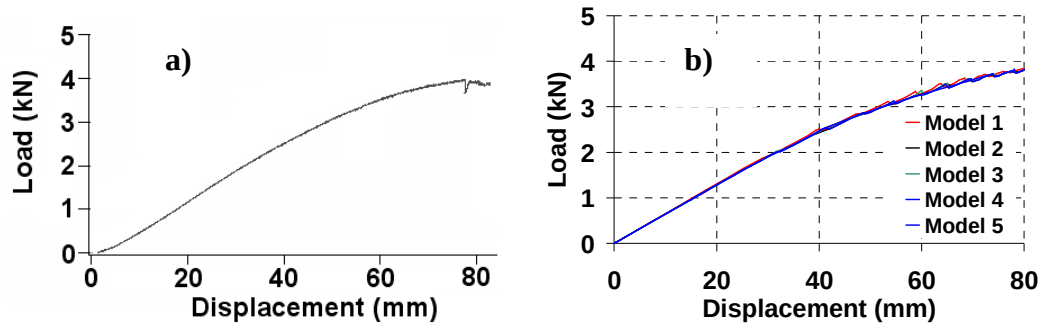

Figure 5. Load-displacement curves – a) Experiment [5]; b) FE models

Delamination

The damage initiation criterion and the delamination growth are investigated along the holes edges. The polar position used is referring to the position of the nodes as described in Figure 6.

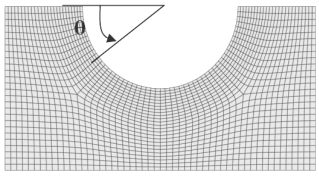

Figure 6. Nodal cylindrical coordinate system at the periphery of the hole

Delamination initiation

The delamination initiation load (i.e. the load at which $\delta = \Delta^0$) is investigated for all FE models. In models where cohesive layers are studied separately (models 1-4), the damage criteria is fulfilled at 0.7 kN, 0.9 kN, 0.7kN and 0.45 kN for the models with cohesive elements positioned at interfaces 1, 2, 3 and 4 respectively. In the model where four cohesive layers are considered (model 5), damage onset is predicted in cohesive layers at interfaces 1, 2 and 4 at 0.9 kN. The criterion is fulfilled at a load of 1.0 kN at interface 3. Consequently, model 5 predicts damage initiation at slightly higher loads than models 1-4, which only consider delamination at a single interface.

The predicted angle, θ, where delamination initiates varies slightly between models 2-5 and 3-5. The results are reported in table 4. The discrepancies are however small enough to consider that prediction is not influenced by the number of cohesive layers.

Table 4. Delamination initiation: angular position (θ)

Interface	Model 1	Model 2	Model 3	Model 4	Model 5
1	66° and 114°	-	-	-	66° and 113°
2	-	90°	-	-	104°
3	-	-	104°, then 63° dominant	-	62°
4	-	-	-	73°	74°

Delamination growth

The delamination growth is monitored in ABAQUS by controlling the value of the stiffness degradation, which takes the value 1 at $\delta = \Delta^f$ (see Figure 1).

Figure 7 shows contour plots of the delamination growth for each cohesive layer at 3.8 kN. If comparing these contour plots, it can be shown that the damaged area is smaller in the cohesive layers of the model with 4 cohesive layers (highly damaged area are represented in dark grey).

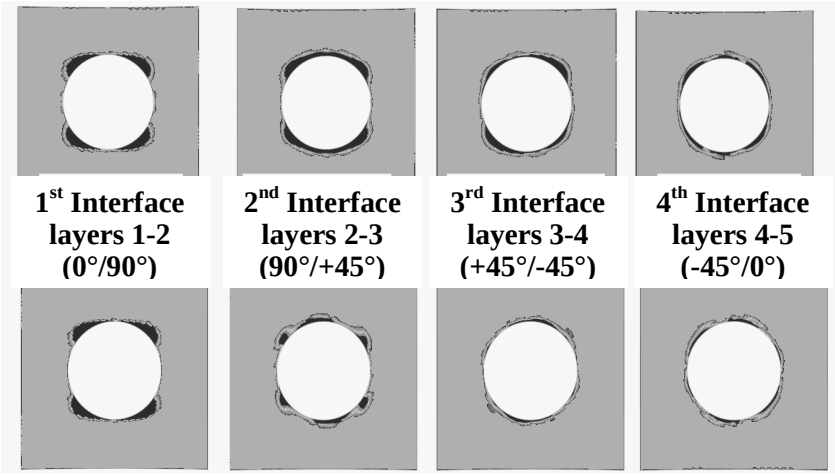

Figure 7. Delamination growth around the hole at P = 3.8 kN. Models with one cohesive layer on the upper line, and model with 4 cohesive layers on the lower line

It was verified that the size of the cohesive elements does not influence the structural response of the laminate.

The delamination initiation at maximum load is investigated from the results of the element size parametric study. Paths are created around half the circumference of the hole (Figure 6). The stiffness degradation at the edge of the hole, as a function of the polar position of the nodes is plotted in Figure 8-a. All models predict delamination growth in the region ranging from $\theta \approx 45°$ to $\theta \approx 135°$. Only an increase of the stiffness degradation, from 0.78 to 0.85, due to higher stress level in smaller elements, is registered close to the 0° and 180° polar positions.

The shear stresses have been plotted along a path created in the areas where large delamination is observed. As expected, the shear stress slightly increases while decreasing the element size. The shear stress level at the edge of the hole, where elements are almost fully damaged is slightly lower in the model with 0.125 mm element size. Additionally, it can be noticed that the shear stress decreases along a shorter distance after the peak value is reached while decreasing the element size (Figure 8-b), which means that higher stresses are predicted ahead the crack tip when coarser mesh is used.

The element size parametric study shows that there is no need in this particular case to use element smaller than 0.5 mm, since no significant differences have been observed. An explanation is the predominance of mode II, where larger cohesive zone allow

coarser mesh to be used. The mode mix ratio, β, is estimated to be greater than 95 % (see Equation 2).

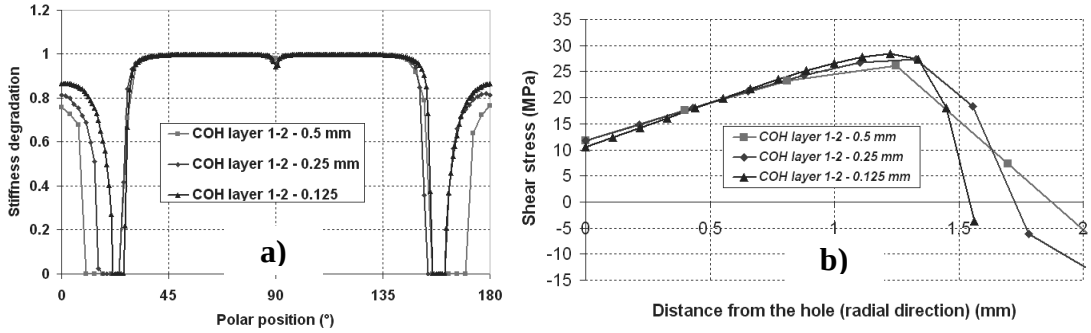

Figure 8. a) Delamination around the hole at P=3.8 kN and b) shear stresses along a radial path where first delamination occurs

COMPARISON WITH EXPERIMENTAL OBSERVATIONS

Some results of the fractography analysis carried out in [5] are reported in Figure 9. Delaminations were observed between multiple layers at the tension side (between layers 1-2, layers 2-3, layers 4-5, layers 7-8 and layers 9-10 (see Figure 8 in [5]).

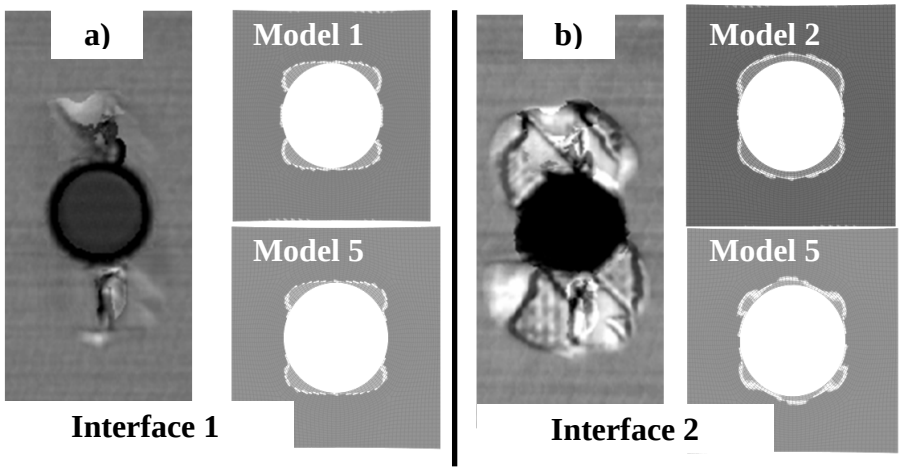

Figure 9. a) Damage observed by ultrasonic C-Scan microscopy at interface 1 and b) interface 2. Predicted damage from FE models are shown on the right.

From the ultrasonic C-scan study, the size and the direction in which the damage propagates are clearly identified. Figure 9-b shows an extensive delamination damage area at the second interface, i.e. between 90° and 45° layers. Delamination have grown in the transverse direction to the load, with a delaminated area extended 20 mm from the hole edges at a maximum load of 3.9 kN. The results from the FE models 1, 2 and 5 show delamination direction of growth in good agreement with the experiment. However, the size of the delaminated area, which is represented in light grey in Figure 9, is much smaller, extended at its maximum 2 to 3 mm from the edges of the notch.

Regarding the comparison between FE model 5 and FE models 1, 2, 3 and 4, it can be seen that the number of cohesive layers being modelled influence the amount of damage and the size of the delamination at similar load levels. This is resulting from the distribution of damage in all cohesive layer in model 5, while damage is concentrated in one cohesive layer only for models 1 to 4.

The FE models conducted in this study underestimate the damage area compared to the experimental results. The difference can be explained by the fact that intralaminar damage like matrix cracking, which contributes to the delamination process, has not been addressed as a possible damage mechanism in the present FE study. Shear cracks are observed in the first 90° layer on the tension side [5]. These cracks run through the layer and delaminations are observed on both sides of the layer (between the layers 1 and 2 and layers 2 and 3). Another explanation is the modelling of all cohesive layers using fracture toughness values for delamination in unidirectional laminates (i.e. 0°/0°). The laminate used in the study shows delaminations between layers with different orientation angle where the fracture energy may be lower [6], which influence the delamination onset and growth.

A particular feature of delamination in multidirectional laminates, not considered in this study, is the possibility for the crack to migrate from one interface to another, since the change in fibre orientation does not confine the crack at the interface where it initiated [7]. This delamination mechanism (multi-plane delamination) interacts with intralaminar damage. Without considering it, the delamination has no longer the possibility to grow through the weakest region of the laminate. This artificial restriction would probably yield accurate results for particular loading modes and laminate lay-up, where in-plane damage is not a driving damage mode. In the present case of notched multidirectional laminates loaded in bending, considering delamination only is not sufficient.

Previous papers [8-9] have pointed out the complexity of predicting interacting intralaminar and interlaminar damage growth. The finite element models are either conducted by implementing user-defined commands in finite element codes, or restricted to predefinition of possible failure regions.

CONCLUSION

The delamination onset and growth in notched composite laminates has been investigated using finite element analysis and compared to experimental results. From experimental C-scan and microscopic study of a tested specimen presented in an accompanying paper, the delaminated and damaged areas were determined. Cohesive elements have been used to model delamination onset and growth between the observed delaminated layers of the notched laminate under flexural load.

The influence of the number of delaminated areas modelled is shown by five different models with either cohesive elements positioned between different layers or with cohesive elements positioned between all layers subjected to delamination. The models with only one cohesive layer show different results than the model with four cohesive layers in terms of the size of the delaminated area. No significant influence on the load displacement curves is noticed. The delamination process is probably too local to globally influence the behaviour of the composite plate.

The element size parametric study showed that there is no need in this particular case to use element smaller than 0.5 mm, since no significant differences in terms of load-displacement behaviour, size of the damage area or stresses have been observed. All models predict delamination to initiate in the region ranging from $\theta \approx 66°$ to $\theta \approx 114°$. Predicted position of delamination initiation and direction of growth correspond to experimental observations for all models. However, the extent of delamination growth is significantly underestimated for the second interface (90º/45º) on the tension loaded side. This discrepancy may be explained by an overestimate of the fracture toughness for the 90º/45º interface, employing fracture toughness data for a 0º/0º interface.

In-plane damage like matrix cracking occurs prior to delamination and was also observed experimentally. It is therefore not enough to consider a FE model with only cohesive element to model the delamination process in notched composite plate. There is a need to model simultaneously progressive damage and delamination to accurately capture damage initiation and growth in notched composite plate under flexural loading. To predict final collapse it is also necessary to include in-plane fiber failure.

ACKNOWLEDGEMENTS

This project was conducted at Swerea Sicomp AB, in collaboration with Saab Aerostructures and the Swedish Defence Research Agency (FOI). The authors gratefully acknowledge the financial support provided by Vinnova within the Swedish National Aeronautical Research Program (NFFP).

REFERENCES

[1] Nyman T., “Fatigue and Residual strength of Composite Aircraft Structures”, Doctoral Thesis, Royal Institute of Technology, ISSN 0280-4646, 1999

[2] Camanho, P. P., and C. G. Davila, “Mixed-Mode Decohesion Finite Elements for the Simulation of Delamination in Composite Materials,” NASA/TM-2002–211737, pp. 1–37, 2002.

[3] Benzeggagh, M. L., and M. Kenane, “Measurement of Mixed-Mode Delamination Fracture Toughness of Unidirectional Glass/Epoxy Composites with Mixed-Mode Bending Apparatus,” Composites Science and Technology, vol. 56, pp. 439–449, 1996

[4] ABAQUS version 6.7-1 ”User manual” Abaqus Inc., 2007

[5] Nilsson S., Bredberg A. and Asp, L.E., “Size Effects on Strength of Notched CFRP Laminates Loaded in Bbending”, Proceeding of the 17th International Conference on Composite Materials (ICCM17), Edinburg, UK, 2009

[6] Gordniana K., Hadaviniaa H., Masona P.J. and Madenci E., “Determination of fracture energy and tensile cohesive strength in Mode I delamination of angle-ply laminated composites”, Composite Structures vol. 82, pp. 577-586, 2008

[7] Singh S. and Greenhalgh E., “Micromechanisms of Interlaminar Fracture in Carbon-Epoxy Composites at Multidirectional Ply Interfaces”, 4th Int. Conf. on Deformation and Fracture of Composites, Manchester, UK, 1997

[8] Kashtalyana M. and Soutis C., “Analysis of Composite Laminates with Intra- and Interlaminar damage”, Progress in Aerospace Sciences vol. 41 pp. 152–173, 2005

[9] Hallett S.R., Green B.G., Jiang W.G., Wisnom M.R., “An Experimental and Numerical Investigation into the Damage Mechanisms in Notched Composites”, Composites: Part A vol. 40 pp. 613–624, 2009